Journal of Radiation Research, Vol. 58, No. 3, 2017, pp. 302–312
doi: 10.1093/jrr/rrw110
Advance Access Publication: 14 December 2016

Modeling cell survival and change in amount of DNA during protracted irradiation

Yusuke Matsuya[1], Kaori Tsutsumi[2], Kohei Sasaki[3], Yuji Yoshii[4], Takaaki Kimura[1] and Hiroyuki Date[2*]

[1]Graduate School of Health Sciences, Hokkaido University, Kita-12, Nishi-5, Kita-ku, Sapporo 060-0812, Japan
[2]Faculty of Health Sciences, Hokkaido University, Kita-12, Nishi-5, Kita-ku, Sapporo 060-0812, Japan
[3]Faculty of Health Sciences, Hokkaido University of Science, Maeda 7-15, Teine-ku, Sapporo 006-8585, Japan
[4]Biological Research, Education and Instrumentation Center, Sapporo Medical University, Minami-1, Nichi-17, Chuo-ku, Sapporo 060-8556, Japan
*Corresponding author. Faculty of Health Sciences, Hokkaido University, Kita-12, Nishi-5, Kita-ku, Sapporo 060-0812, Japan.
Tel: +81-11-706-3423; Fax: +81-11-706-4916; Email: date@hs.hokudai.ac.jp
Received June 20, 2016; Revised August 30, 2016; Editorial Decision October 8, 2016

ABSTRACT

Hyper-radiosensitivity (HRS) is a well-known bioresponse under low-dose or low-dose-rate exposures. Although disorder of the DNA repair function, non-targeted effects and accumulation of cells in G_2 have been experimentally observed, the mechanism for inducing HRS by long-term irradiation is still unclear. On the basis of biological experiments and a theoretical study, we have shown that change in the amount of DNA associated with accumulation of cells in G_2 enhances radiosensitivity. To demonstrate continuous irradiation with 250 kVp X-rays, we adopted a fractionated regimen of 0.186 or 1.00 Gy per fraction at intervals of 1 h (i.e. 0.186 Gy/h, 1.00 Gy/h on average) to Chinese Hamster Ovary (CHO)-K1 cells. The change in the amount of DNA during irradiation was quantified by flow cytometric analysis with propidium iodide (PI). Concurrently, we attempted a theoretical evaluation of the DNA damage by using a microdosimetric-kinetic (MK) model that was modified to incorporate the change in the amount of DNA. Our experimental results showed that the fraction of the cells in G_2/M phase increased by 6.7% with 0.186 Gy/h and by 22.1% with 1.00 Gy/h after the 12th irradiation. The MK model considering the change in amount of DNA during the irradiation exhibited a higher radiosensitivity at a high dose range, which could account for the experimental clonogenic survival. The theoretical results suggest that HRS in the high dose range is associated with an increase in the total amount of DNA during irradiation.

KEYWORDS: dose-rate effects, protracted irradiation, surviving fraction, accumulation of cells in G_2, amount of DNA, microdosimetric-kinetic model

INTRODUCTION

Effects of low-dose (below 0.5 Gy) or low-dose-rate irradiation on mammalian tissues have recently been highlighted. After the accident at the Fukushima Daiichi Nuclear Power Station in 2011, particularly close attention has been paid to low-dose and low-dose-rate radiation effects in relation to protection of human health [1]. The focus has been on the bio-effects of irradiation at a low dose or lower dose rate, and hyper-radiosensitivity (HRS) has been reported [2–4] [sometimes referred to as 'inverse dose-rate effects' (IDREs)] under continuous irradiation [5, 6]. IDREs were observed not only in the form of mutations or chromosomal aberrations [7, 8] but also in cell viability (clonogenic survival) [9]. Biological experiments suggest some potential causes of IDREs (low-dose-rate HRS), such as accumulation of cells in G_2 phase during protracted irradiation [9, 10], functional disorder of DNA repair with low dose irradiation [11–13] and non-targeted effects (so-called 'bystander effects') [14–16]. However, the mechanism for inducing IDREs is still unclear. Estimating the contribution due to each cause is crucial if we are to clarify the mechanism for IDREs.

For evaluating the surviving fraction of cells after irradiation, the microdosimetric-kinetic (MK) model was proposed by Hawkins [17, 18], and it has been used in the fields of radiation biology and radiotherapy [19–22]. This model considers the number of DNA double-strand breaks (the main factor leading to cell death) induced by

ionizing radiation [18, 19]. By solving rate equations for the numbers of potentially lethal lesions (PLLs) and lethal lesions (LLs), the relation between absorbed dose (D) and cell surviving fraction can be deduced by considering energy depositions around radiation particles (microdosimetry) [19, 23] and dose-rate effects (DREs) [18, 20, 24]. Previously, based on experimental data, we proposed an MK model that takes account of several types of irradiation schemes, such as single-dose instantaneous irradiation, split-dose irradiation and continuous irradiation [18, 22, 24]. However, the model which we previously used for evaluating the DREs did not consider the condition of the amount of DNA, which is dependent upon the cell cycle during protracted irradiation; thus, the DREs need to be re-evaluated after improvement of the MK model so as to incorporate the amount of DNA associated with the accumulation of cells in G_2 during protracted irradiation.

DREs have usually been investigated experimentally using mammalian cell lines in the plateau phase [8, 25]. The plateau phase represents the situation in the majority of cells in most biotissues. In plateau phase, the cell population consists mainly of cells in the G_0 or G_1 phase (e.g. 80% of the cells are in G_1 phase) [26]. Some biological experiments have clearly shown the modulations in the radiosensitivity for every phase of cell cycle in cultured mammalian cells [27, 28]. Cell survival during the period of G_2 tends to be lower than that in G_1 [28], which may be because the DNA damage is enhanced by doubling the amount of DNA, in spite of the high repair efficiency of homologous recombination (HR) [29]. Therefore, a shift in the cell population ratio of the G_1 to G_2 phases may enhance radiosensitivity at the endpoint of cell survival. The phase difference of the cell in terms of the amount of DNA was incorporated into the MK model [30], which enabled us to consider the change in the average amount of DNA per nucleus triggered by accumulation of cells in G_2. To our knowledge, there have been few trials that compared the measured cell viability with theoretical studies concerning the amount of DNA and the kinetics of DNA lesions (DNA repair and transformation of PLLs into LLs) during irradiation.

The purpose of this study was to investigate cell survival curves, focusing on accumulation of cells in the G_2 phase for two dose rates, 1.00 Gy/h and 0.186 Gy/h, by using an improved MK model. In terms of biological experiments and theoretical evaluation, we evaluated how accumulation of cells in G_2 exerts an influence on cell viability under protracted irradiation. This model study gives us some clues about the mechanism for IDREs on cell survival.

MATERIALS AND METHODS

Methodology in the MK model

A cell nucleus is assumed to consist of a few hundred micro territories, called domains. For simplicity, the domain is generally defined as a sphere with diameter from 1.0 to 2.0 μm [18–21]. When ionizing radiation transfers its energy into a cell domain, PLLs may be induced. In the MK model used here, a PLL is assumed to undergo one of three transformations until the time t_r [h]: (i) a PLL may transform into a LL via a first-order process at a constant rate a, (ii) two PLLs may transform into a LL via a second-order process at a constant rate b_d, (iii) a PLL may be repaired via a first-order process at a constant rate c [18–22].

Energy is absorbed into domains along the track of electrons generated by the incident X-rays. The absorbed dose per domain is randomly distributed over all domains. Let z be a dose value to one of the domains, called the specific energy (in Gy). A number of PLLs are created in proportion to the specific energy and the amount of DNA in the domain. If the mass of DNA per domain is denoted by g, which varies from domain to domain according to the cell phase [20, 30], the number of PLLs in the domain as a function of time after irradiation, $x_d(t)$, is described by

$$\frac{\mathrm{d}}{\mathrm{d}t}x_d(t) = -(a + c)x_d(t) - 2b_d x_d(t)^2. \tag{1a}$$

However, since the second term on the right-hand side is usually negligibly small compared with the first term [18],

$$\frac{\mathrm{d}}{\mathrm{d}t}x_d(t) \cong -(a + c)x_d(t). \tag{1b}$$

This can be solved as

$$x_d(t) = k_d g z e^{-(a+c)t}, \tag{2}$$

where $k_d gz$ is the average number of PLLs per domain. The number of LLs in the domain, w_d, can be expressed as the following rate equation,

$$\frac{\mathrm{d}}{\mathrm{d}t}w_d = a x_d(t) + b_d x_d(t)^2. \tag{3}$$

Equations 2 and 3 are used for the kinetics of the number of PLLs and LLs in the domain.

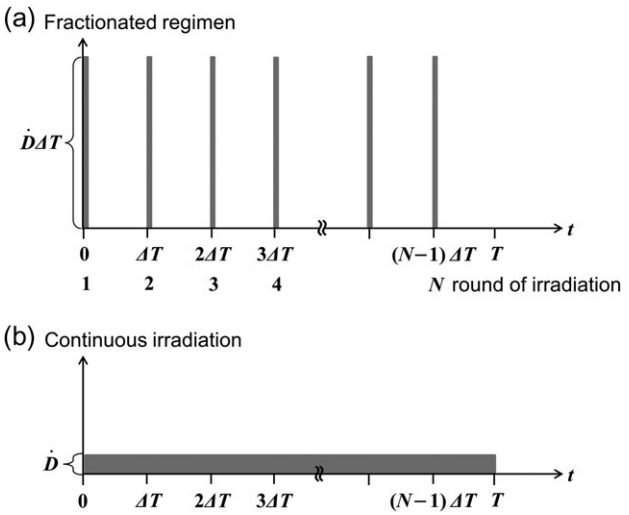

Figure 1 Schematic of irradiation regimen: (a) for fractionated irradiation with dose $\dot{D}\Delta T$ (Gy) at interval ΔT (h) and (b) for continuous irradiation at dose rate $\dot{D}$ (Gy/h). In the MK model, it is assumed that the dose is absorbed discontinuously into the cells. For simplicity, the irradiation time T is divided into N sections [22], and the low-dose-rate continuous irradiation is made of infinite fractionations at a low dose.

Continuous irradiation and the MK model including the amount of DNA

For irradiating biocells to a prescribed dose level, an irradiation period of time is necessary, depending on dose rate. Here we suppose that the population is exposed to radiation for the irradiation time T (h), but the energy is absorbed discontinuously into each domain. If the irradiation time T is divided into N sections, we have the relationship $T = N\Delta T$, where ΔT is a constant period of time [22]. As described in Fig. 1a and b, in the present study we assume that the continuous irradiation is equivalent to a multi-fractionated irradiation with a dose per fraction. Let $z_1, z_2, \ldots, z_N$ and $g_1, g_2, \ldots, g_N$ be the specific energy and the amount of DNA in a domain at each period, $0\sim\Delta T$, $\Delta T\sim 2\Delta T, \ldots, (N-1)\,\Delta T\sim N\Delta T$, respectively. Thus, the number of PLLs per domain is given (using Eq. 2) as:

$$
\begin{aligned}
x_d(t) &= k_d g_1 z_1 e^{-(a+c)t} && [0 \le t < \Delta T]\\
x_d(t) &= \sum_{n=1}^{2} k_d g_n z_n e^{-(a+c)(t-(n-1)\Delta T)} && [\Delta T \le t < 2\Delta T]\\
&\vdots\\
x_d(t) &= \sum_{n=1}^{N-1} k_d g_n z_n e^{-(a+c)(t-(n-1)\Delta T)} && [(N-2)\Delta T \le t < (N-1)\Delta T]\\
x_d(t) &= \sum_{n=1}^{N} k_d g_n z_n e^{-(a+c)(t-(n-1)\Delta T)} && [(N-1)\Delta T \le t < t_r]\\
x_d(t) &= \sum_{n=2}^{N} k_d g_n z_n e^{-(a+c)(t-(n-1)\Delta T)} && [t_r \le t < t_r + \Delta T]\\
x_d(t) &= \sum_{n=3}^{N} k_d g_n z_n e^{-(a+c)(t-(n-1)\Delta T)} && [t_r + \Delta T \le t < t_r + 2\Delta T]\\
&\vdots\\
x_d(t) &= \sum_{n=N-1}^{N} k_d g_n z_n e^{-(a+c)(t-(n-1)\Delta T)} && [t_r + (N-3)\Delta T \le t < t_r + (N-2)\Delta T]\\
x_d(t) &= k_d g_N z_N e^{-(a+c)(t-(N-1)\Delta T)} && [t_r + (N-2)\Delta T \le t < t_r + (N-1)\Delta T]\\
x_d(t) &= 0. && [t_r + (N-1)\Delta T \le t] \qquad (4)
\end{aligned}
$$

Next, by substituting Eq. 4 into Eq. 3 and integrating the rate equation for LL over each period of time, the integrated number of LLs in the domain is deduced as:

$$
\begin{aligned}
w_d = {} & \left[\frac{ak_d}{(a+c)} + \frac{ck_d}{(a+c)} e^{-(a+c)t_r}\right] \sum_{n=1}^{N} (g_n z_n)\\
& + \frac{b_d {k_d}^2}{2(a+c)}\left[1 - e^{-2(a+c)t_r}\right] \sum_{n=1}^{N} (g_n^2 z_n^2) + \frac{b_d {k_d}^2}{2(a+c)}\left[1 - e^{-2(a+c)t_r}\right]\\
& \times \left\{ \frac{2}{\left[1 - e^{-2(a+c)t_r}\right]} \sum_{n=1}^{N-1} \sum_{m=n+1}^{N} \left[e^{-(m-n)(a+c)\Delta T}\right.\right.\\
& \left.\left. - e^{-(a+c)(2t_r-(m-n)\Delta T)}\right] g_n g_m z_n z_m \right\}. \qquad (5)
\end{aligned}
$$

Then, assuming that t_r is infinite, as discussed by Hawkins [20], Eq. 5 can be approximated by:

$$
\begin{aligned}
w_d = {} & A \sum_{n=1}^{N} (g_n z_n) + B \sum_{n=1}^{N} \left(g_u^2 z_n^2\right)\\
& + B\left\{ 2 \sum_{n=1}^{N-1} \sum_{m=n+1}^{N} \left[e^{-(m-n)(a+c)\Delta T}\right] g_n g_m z_n z_m \right\}, \qquad (6)
\end{aligned}
$$

where $A = \frac{ak_d}{(a+c)}$ and $B = \frac{b_d {k_d}^2}{2(a+c)}$.

Let $\langle w \rangle$ be the average number of LLs per cell nucleus and $\langle w_d \rangle$ the average number of w_d per domain, thus $\langle w \rangle$ and $\langle w_d \rangle$ can be linked as:

$$
\begin{aligned}
\langle w \rangle = {} & \sum_{i=1}^{p} \langle w_d \rangle\\
= {} & \sum_{n=1}^{N} \left[A \langle G_n \rangle \int_0^\infty z_n f(z_n)\,\mathrm{d}z_n \right.\\
& \left. + B' \langle G_n \rangle^2 \Phi_n \int_0^\infty {z_n}^2 f(z_n)\,\mathrm{d}z_n \right]\\
& + 2B' \sum_{n=1}^{N-1} \sum_{m=n+1}^{N} \left\{ \left[e^{-(m-n)(a+c)\Delta T}\right] \langle G_n \rangle \langle G_m \rangle \right.\\
& \left. \times \int_0^\infty z_n f(z_n)\,\mathrm{d}z_n \int_0^\infty z_m f(z_m)\,\mathrm{d}z_m \right\}. \qquad (7)
\end{aligned}
$$

Here, p is the average number of domains per cell nucleus, $f(z_n)$ is the probability density of the specific energy for each period, $\langle G_n \rangle = p\langle g_n \rangle$ is the amount of DNA per cell nucleus, and $B' = B/p$, $\Phi_n = \langle g_n^2 \rangle / \langle g_n \rangle^2$ is a dimensionless parameter. Assuming that $\langle z_n \rangle$ is the average dose to a cell for period ΔT (h) and the absorbed dose rate is constant during the total irradiation time T (h) ($\langle z_1 \rangle = \langle z_2 \rangle = , \ldots, = \langle z_n \rangle = \dot{D}\Delta T$), we have:

$$
\begin{aligned}
\langle w \rangle = {} & \sum_{n=1}^{N} \left[\left(A \langle G_n \rangle + \gamma B' \langle G_n \rangle^2 \Phi_n\right) \dot{D}\Delta T + B' \langle G_n \rangle^2 \Phi_n (\dot{D}\Delta T)^2 \right]\\
& + 2B' \left\{ \sum_{n=1}^{N-1} \sum_{m=n+1}^{N} \left[e^{-(m-n)(a+c)\Delta T}\right] \langle G_n \rangle \langle G_m \rangle \right\} (\dot{D}\Delta T)^2, \qquad (8)
\end{aligned}
$$

where

$$
\langle z_n \rangle = \int_0^\infty z_n f(z_n)\,\mathrm{d}z_n = \dot{D}\Delta T, \qquad (9a)
$$

$$
\int_0^\infty {z_n}^2 f(z_n)\,\mathrm{d}z_n = \langle z_n \rangle^2 + \frac{y_D}{\rho \pi {r_d}^2} \langle z_n \rangle = (\dot{D}\Delta T)^2 + \gamma \dot{D}\Delta T. \qquad (9b)
$$

$\dot{D}$ is the constant absorbed dose rate (Gy/h), y_D is the dose-mean lineal energy (keV/μm) as the microdosimetric parameter, ρ and r_d are the density and radius of the domain [$\rho = 1.0$ (g/cm^3) and $r_d = 0.5$ (μm)], respectively. To write Eq. 8 compactly, we define:

$$
\alpha_n = A \langle G_n \rangle, \qquad (10a)
$$

$$
\beta_n = B' \langle G_n \rangle^2 \Phi_n, \qquad (10b)
$$

$$\beta_{nm} = B' \langle G_n \rangle \langle G_m \rangle. \tag{10c}$$

Assuming that the number of LLs per nucleus follows the Poisson distribution, the expression of cell surviving fraction (S) is given by the fraction of clonogenic cells having no LL as:

$$\begin{aligned}\langle w \rangle &= \sum_{n=1}^{N} [(\alpha_n + \gamma\beta_n)\dot{D}\Delta T + \beta_n(\dot{D}\Delta T)^2] \\ &\quad + 2\sum_{n=1}^{N-1}\sum_{m=n+1}^{N} \{\beta_{nm}[e^{-(m-n)(a+c)\Delta T}]\}(\dot{D}\Delta T)^2 \\ &= -\ln S. \end{aligned} \tag{11}$$

Equation 11 represents the cell surviving fraction, including the change in amount of DNA during irradiation, $<G_1>$, $<G_2>$,…, $<G_n>$. The relative amount of DNA in the cell nucleus is supposed to correspond to the relative amount of DNA measured by means of staining DNA in the nucleus with propidium iodide (PI) or DAPI [31].

Conformance of the MK model to the previous continuous irradiation model

If we neglect the change in amount of DNA during the cell cycle (i.e. $\alpha_n = \alpha_0$ = constant and $\beta_n = \beta_{nm} = \beta_0$ = constant) and take the limit N to infinity, the expression in Eq. 11 is transformed as follows:

$$\begin{aligned}&\lim_{N\to\infty}(-\ln S) \\ &= \lim_{N\to\infty}\sum_{n=1}^{N}[(\alpha_0 + \gamma\beta_0)\dot{D}\Delta T + \beta_0(\dot{D}\Delta T)^2] \\ &\quad + 2\lim_{N\to\infty}\sum_{n=1}^{N-1}\sum_{m=n+1}^{N}\{\beta_0[e^{-(m-n)(a+c)\Delta T}]\}(\dot{D}\Delta T)^2 \\ &= (\alpha_0 + \gamma\beta_0)\dot{D}T + \beta_0\left\{\frac{2}{(a+c)^2T^2}[(a+c)T + e^{-(a+c)T} - 1]\right\}\dot{D}^2T^2.\end{aligned}$$

Thus, we have

$$-\ln S = (\alpha_0 + \gamma\beta_0)D + F\beta_0 D^2, \tag{12}$$

where

$$F = \frac{2}{(a+c)^2T^2}[(a+c)T + e^{-(a+c)T} - 1] \tag{13}$$

$$D = \dot{D}T. \tag{14}$$

Here, D is the accumulated absorbed dose (Gy). Equation 12 corresponds to the surviving fraction formula with the Lea–Catcheside time-factor [24, 32]. In consideration of the discrete deposition of the energy by electrons into the domain, we regarded the coefficient of D as a constant value independent of the irradiation time T because the single particle pathway can cause an instantaneous pairwise combination of PLLs per domain. In contrast, the coefficient of D^2 is affected by T because this process is induced by the combination of PLLs along two different particle pathways in a non-coincident fashion.

Cell culture and irradiation conditions

In order to investigate the responses of cells exposed to protracted irradiation in terms of the amount of DNA per nucleus and clonogenic survival, we used the Chinese hamster ovary (CHO)-K1 cell line, obtained from RIKEN Bio Resource Center, Japan (RCB0285). The cell culture was maintained in Dulbecco's modified Eagle's medium (DMEM, Sigma Life Science) with 10% fetal bovine serum (FBS, Nichirei Biosciences Inc., Tokyo, Japan) at 37 °C in a humidified 95% air and 5% CO_2 incubator. A population of 4×10^5 cells was seeded on the cell culture dish with ϕ 60 mm (Nippon Genetics) and cultured for 4 days to obtain a confluent monolayer in the plateau phase.

As the standard radiation, 250 kVp X-rays (Stabilipan, Siemens, Concord, CA) were applied. We measured the dose rate in air at the surface of the cell culture (using a Farmer-type ionization chamber model NE2581, Nuclear Enterprises Ltd) and determined the dose rate and absorbed dose in water according to TRS 277 [33]. Based on the assumption that continuous irradiation with a low dose rate is the ultimate form of infinite fractionation with impulse-like irradiation [6], the cells were irradiated with 1.00 Gy or 0.186 Gy (1.00 Gy/min or 0.186 Gy/min for 1 min) per fraction at 1 h intervals [$\dot{D}\Delta T$ = 1.00 or 0.186 (Gy), ΔT = 1.0 (h)], i.e. the conditions as illustrated in Fig. 1a.

Flow cytometric analysis of amount of DNA stained with propidium iodide

During the time in each fraction for 0, 2, 4, 6, 8, 10 and 12 h, 10^6 cells in phosphate-buffered saline (PBS)(–) (0.5 ml) were fixed with 70% ethanol (4.5 ml) and kept at 4°C for at least 2 h. After a centrifugation, the cells were resuspended in 1 ml of PBS(–). The cells in suspension were then centrifuged again, and the DNA in the cell nucleus was stained in 0.5 ml FxCycle™ PI/RNase staining solution (Life Technologies) with 0.2% v/v triton X for 15–30 min in the dark at room temperature.

The DNA stained with PI was measured by using the Attune acoustic focusing flow cytometer (Applied Biosystems by Life Technologies TM). The intensity was normalized by that of cells in G_0/G_1 phase. In addition, the fractions of the cells in G_0/G_1, S and G_2/M phases were measured from the histogram of the amount of DNA, assuming that the distributions for the G_0/G_1 and G_2/M phases were Gaussian.

Clonogenic survival assay

After irradiation following the regimen with 1.00 Gy per fraction, the cells were trypsinized and their number was counted. Next, the cells in the optimal number were reseeded on the ϕ 60 mm cell culture dish (Nippon Genetics) and cultured in a CO_2 incubator. After culturing for 10 days, the cells were fixed with methanol directly and stained with 2% Giemsa solution (Kanto Chemical Co. Inc., Tokyo, Japan). The number of colonies per dish was counted, and the survival rate was determined by the plating efficiency of the non-irradiated cells. Finally, the relationship between the integral absorbed dose (Gy) and log S was obtained.

Description of the cell survival curve with change in amount of DNA

To evaluate the contribution of the change in amount of DNA per cell to the cell survival, the relative amount of DNA measured by flow cytometric analysis was incorporated into the MK model expressed in Eq. 11. The relative amount of DNA per cell nucleus at irradiation round n, $<G_n>/<G_1>$ and $<G_n>^2\Phi_n/<G_1>^2\,\Phi_1$, was calculated by

$$\frac{\langle G_n\rangle}{\langle G_1\rangle} = \frac{\int G_n f(G_n)\mathrm{d}G_n}{\int G_1 f(G_1)\mathrm{d}G_1} \tag{15}$$

and

$$\frac{\langle G_n\rangle^2\,\Phi_n}{\langle G_1\rangle^2\,\Phi_1} = \frac{\langle G_n^2\rangle}{\langle G_1^2\rangle} = \frac{\int G_n^2 f(G_n)\mathrm{d}G_n}{\int G_1^2 f(G_1)\mathrm{d}G_1}, \tag{16}$$

where $f(G_n)$ is the probability density of the cells, which have an amount of DNA G_n per nucleus. The relative amount of DNA data for 1.00 Gy/h and for 0.186 Gy/h were curve fitted by an exponential function by the least squares method. The function was then incorporated into the MK model.

The parameters used in this study are listed in Table 1. They were determined by Eqs 12–14 and our previous survival data for a constant rate of irradiation for 10 min [24] as follows:

(i) F for $T = 10$ min was calculated from $(a + c) = 0.704 \pm 0.118$ in Eq. 13,
(ii) $(\alpha_0 + \gamma\beta_0)$ $[= (\alpha_1 + \gamma\beta_1)]$ and β_0 $(= \beta_1)$ were determined by fitting the linear–quadratic formula in Eq. 12 to the cell survival data (for single-dose irradiation for 10 min),
(iii) α_0 $(=\alpha_1)$ was calculated using the parameters $((\alpha_0 + \gamma\beta_0)$, β_0 and $\gamma = 0.924)$.

Before evaluating the effect of amount of DNA during irradiation on the cell survival curve, we confirmed that fractionated irradiation with 1.50, 1.00 and 0.186 Gy per fraction at 1 h intervals is equivalent to continuous irradiation at the rate of 1.50, 1.00 and 0.186 Gy/h, respectively. Then, the cell survival curves taking account of the measured amount of DNA during irradiation (Eq. 11) were depicted in comparison with the curves based on the previous MK model (Eq. 12). Finally, we evaluated the influence of change in amount of DNA during irradiation on the surviving fraction by comparing the curves based on the model with our survival data (fractionated regimen at 1.00 Gy/h on average) and the data reported by Metting et al. (continuous iradiation at 1.50 and 0.186 Gy/h) [34].

Table 1. Parameters in the MK model for the CHO-K1 cell line in the plateau phase

Parameters in the MK model	Values (mean ± sd)
$\alpha_1 = A\langle G_1\rangle$ $(= \alpha_0)$ (Gy^{-1})	0.155 ± 0.027
$\beta_1 = B\langle G_1{}^2\rangle$ $(= \beta_0)$ (Gy^{-2})	0.048 ± 0.003
$(a + c) \fallingdotseq c$ $(\mathrm{h}^{-1})^*$	0.704 ± 0.118
ρ $(\mathrm{g/cm}^3)$	1.000
r_d $(\mu\mathrm{m})$	0.500
$\gamma = y_D/(\rho\pi r_d^2)$ (Gy) (250 kVp X-rays)	0.924

*$(a + c)$ (h^{-1}) can be approximated by c (h^{-1}) because the value a is a few percentage of c [12, 14].

Statistics and model conformance

The difference in the kinetics of cell phase (G_0/G_1, S, G_2/M) from those of the group before irradiation $[t = 0$ (h)] was evaluated by using a multiple comparison method, the Tukey–Kramer test. For evaluating the model conformance to the S and −log S, Chi-square values were calculated by:

$$\chi_S^2 = \sum_{i=1}^{n} \frac{(S_{\mathrm{exp}} - S_{\mathrm{MK}})^2}{S_{\mathrm{MK}}} \tag{17a}$$

$$\chi_{-\log S}^2 = \sum_{i=1}^{n} \frac{(-\log S_{\mathrm{exp}} + \log S_{\mathrm{MK}})^2}{-\log S_{\mathrm{MK}}}, \tag{17b}$$

where S_{exp} is the measured surviving fraction, S_{MK} is the surviving fraction calculated by the MK model, n is the number of data, and χ_S^2 and $\chi_{-\log S}^2$ are the Chi-square values of S and −log of S, respectively.

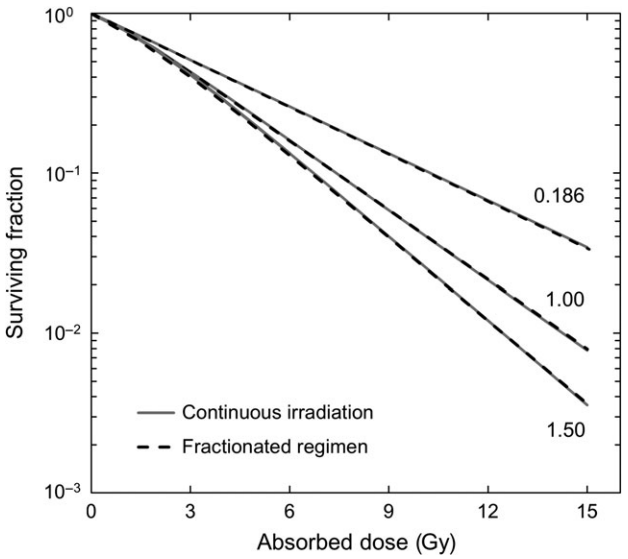

Figure 2. Comparison of fractionated regimens (dotted lines) with 0.186, 1.00 and 1.50 Gy at 1 h intervals with continuous irradiation (solid lines) at 0.186, 1.00 and 1.50 Gy/h according to the theoretical calculation based on Eq. 11 in the MK model for the fractionated regimen and Eqs 12–14 for continuous irradiation. The parameters for the MK model are summarized in Table 1. The number in this figure represents the dose rate in Gy/h. This figure confirms that continuous irradiation is equivalent to fractionated irradiation with pulsed irradiation.

RESULTS AND DISCUSSION

Validation of irradiation regimen for demonstrating continuous irradiation

Before evaluation of the dose-rate effects on biocells, we verified that the approximated design in which the fractionated regimen with pulsed irradiation was equivalent to continuous irradiation. Figure 2 illustrates the dose versus surviving fraction relationship in the fractionated regimen for 1.50, 1.00 and 0.186 Gy at 1 h intervals in comparison with that in continuous irradiation with 1.50, 1.00 and 0.186 Gy/h. The curve for the fractionated regimen was calculated using Eq. 11 in the MK model with a constant amount of DNA during irradiation, and the curve for continuous irradiation was determined using Eqs 12–14. The curves were depicted by theoretical calculations using the MK parameters summarized in Table 1 on the assumption that the amount of DNA is constant during irradiation. The cell survival curves coincide with each other for every integrated dose up to 15 Gy, suggesting that the accumulated number of LLs for fractionated irradiation is the same as that for continuous irradiation. This result justifies the evaluation of the cell survival after irradiation at 0.186 Gy/h and 1.00 Gy/h by means of the fractionated regimen of this study.

Kinetics of the cell cycle and change in the amount of DNA in the cell population during irradiation

Figure 3 shows the probability densities of amount of DNA in the cell population: the left-hand side graphs are for non-exposed cells (control); the central graphs are for 0.186 Gy/h exposure; the right-hand graphs are for 1.00 Gy/h exposure. The probability density was obtained from the flow cytometric data of the DNA histogram. From the DNA histogram given in Fig. 3, we obtained the kinetics of the cell cycle distributions for the control experiment and for protracted exposures (Fig. 4a–c). While there were no significant changes in the cell cycle in the control experiment (Fig. 4a), the fraction of cells in G_2/M phase increased by 6.7% for the 0.186 Gy/h experiment (Fig. 4b) and by 22.1% for the 1.00 Gy/h experiment (Fig. 4c). As shown in Fig. 4, we can detect a subtle accumulation of cells in the

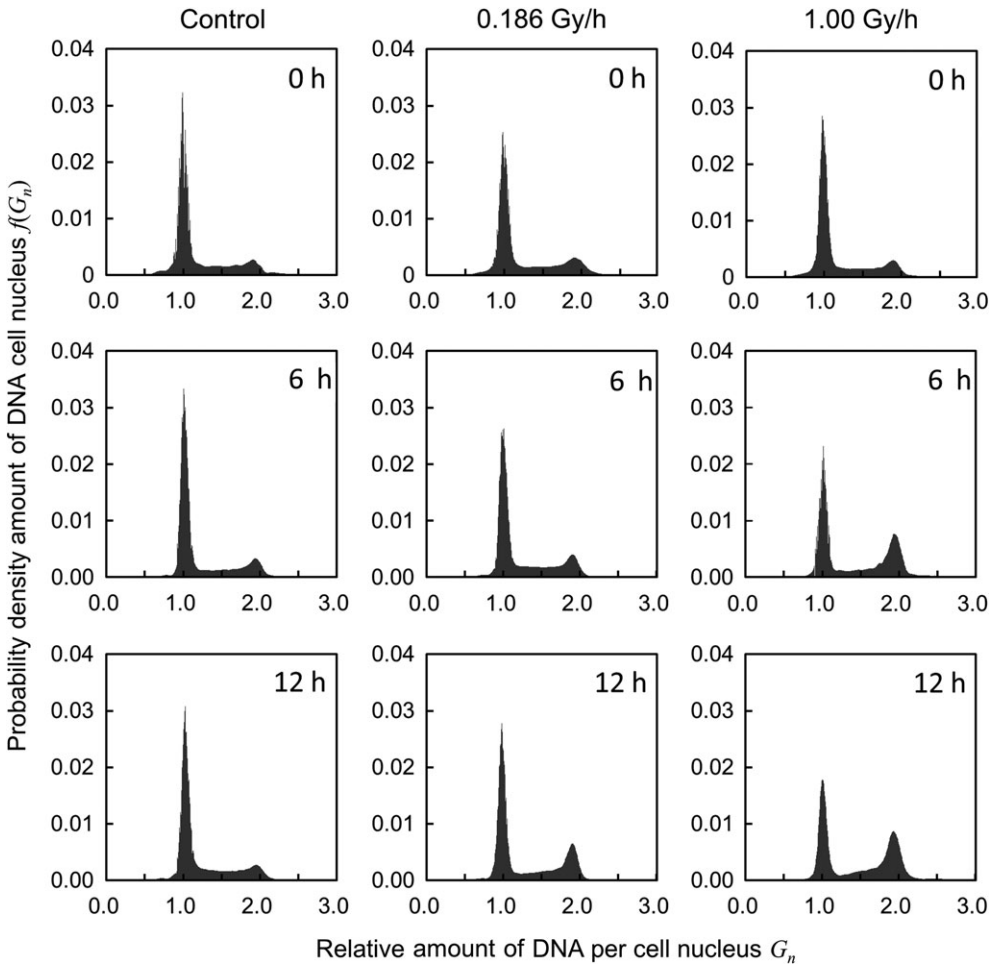

Figure 3. Probability density of the relative amount of DNA per cell nucleus in the CHO-K1 cell line: the left-hand side graphs represent the results of the control experiment (0 Gy) in the contact plateau phase, the central graphs represent the results for 0.186 Gy/fr at 1 h intervals, and the right-hand graphs represent the results for 1.00 Gy/fr at 1 h intervals. DNA was stained with propidium iodide (PI) and measured by using a flow cytometer.

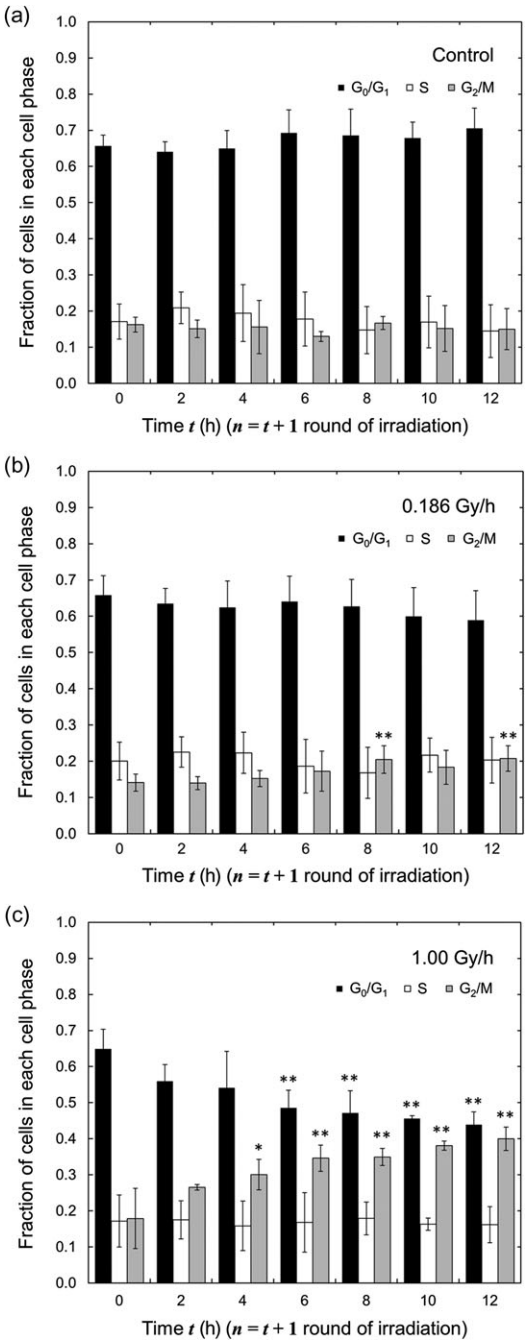

Figure 4. Kinetics of the fractions of the cells in G_0/G_1, S and G_2/M phases during fractionated irradiation. The data were analyzed statistically for the (a) control, (b) 0.186 Gy/h and (c) 1.00 Gy/h experiments. The single asterisks and double asterisks represent $P < 0.05$ and $P < 0.01$ significant differences, respectively. In this figure, we can observe the subtle accumulation of G_2/M cells with 0.186 Gy/h and the significant accumulation with 1.00 Gy/h.

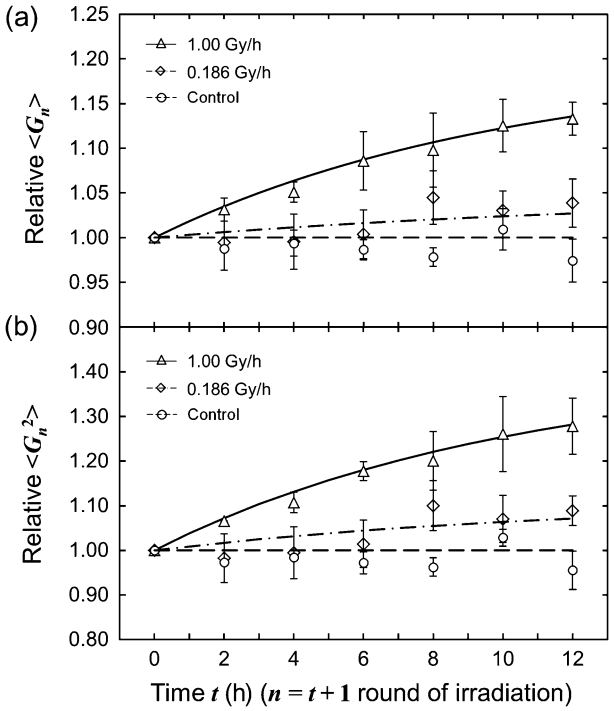

Figure 5. Change in amount of DNA per cell nucleus during irradiation. The relative amounts of DNA $<G_n>/<G_1>$ and $<G_n^2>/<G_1^2>$ were calculated by using the probability density of the amount of DNA shown in Fig. 3 and Eqs 17 and 18. In these figures, the symbols represent the experimentally observed relative amounts of DNA (triangles for 1.00 Gy/h, diamonds for 0.186 Gy/h and circles for control), and the lines are the interpolated curves described by the exponential function. The data were analyzed statistically in the (a) control, (b) 0.186 Gy/h and (c) 1.00 Gy/h experiments. The average amount of DNA in the cell population increased as the fractionation number increased, depending on the magnitude of the dose rate. The bars represent standard errors of the mean.

G_2/M phase under 0.186 Gy/h and a noticeable accumulation under 1.00 Gy/h. According to previous investigations [35, 36], the threshold dose for blocking the progression of the cell cycle at the G_1/S checkpoint is 3.00~5.00 Gy, and the threshold for blocking the progression at the G_2 checkpoint is only 0.09 or 0.20 Gy. On the assumption that 1.0 Gy was absorbed into the cell population per fraction in this experiment, it is inferred that the G_2 checkpoint system was activated, while the G_1/S checkpoint was kept inactivated. On the other hand, 0.186 Gy is a dose value close to the threshold at which the G_2/M checkpoint functions. Our flow cytometric data (Figs 3 and 4) support previous reports on cell cycle checkpoint functioning [35–37].

In regard to the relative amount of DNA in the cell population, the average per nucleus $<G_n>/<G_1>$ and mean-square values $<G_n>^2\Phi_n/<G_1>^2$ Φ_1 are shown in Fig. 5a and b; these values were

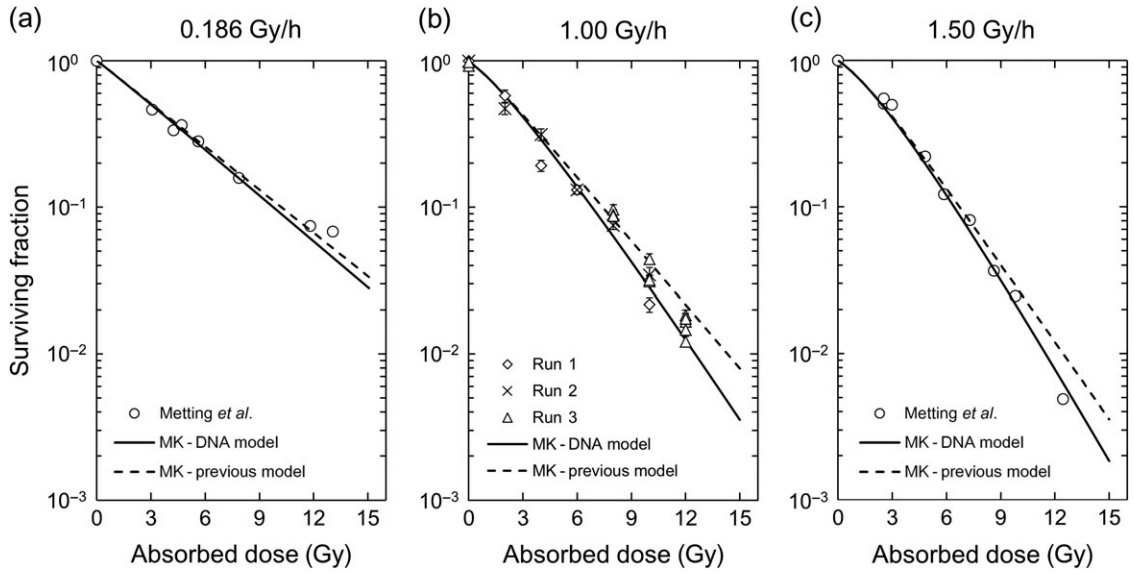

Figure 6. Clonogenic cell survival and cell survival curves calculated by the MK model: (a) **for 0.186 Gy/h,** (b) **for 1.00 Gy/h and** (c) **for 1.50 Gy/h. The symbols (open diamonds, crosses and open triangles) in Fig. 6b represent our experimental survival data, and the open circles in Fig. 6a and 6c represent the data reported by Metting *et al.* [34]. Dotted lines represent the curves described by the previous MK model with constant amounts of DNA, and solid lines represent the curves described by our MK (MK-DNA) model with increases in the amount of DNA. The fidelity of the MK-DNA model was better than that of the previous model (Table 2).**

calculated from the data in Fig. 3, using Eqs 15 and 16 for the present fractionated irradiation regimen. The MK model can describe the kinetics of the DNA damage modified by the change in amount of DNA shown in Figs 3 and 5, and takes account of the numbers of the PLLs and the pairwise combination of PLLs per domain. In Fig. 5a and b, the symbols (triangles for 1.00 Gy/h, diamonds for 0.186 Gy/h and circles for control) represent the experimentally determined relative amounts of DNA, and the lines are the interpolated curves described by the exponential function. Because of there being no significant differences over time for the control experiment, we determined that the relative amount of DNA was unity in the case of control experiment. The results under protracted exposures show that the average amount of DNA in the cell population increases as the fraction number increases, which depends on the magnitude of the dose rate.

Target theory is well known in the field of radiation biology [38, 39]. A salient feature of the present study is that the amount of DNA (associated with the accumulation of cells in G_2) was quantified as the volume of the target per domain or per cell nucleus, which may bring about the possibility of enhancing DNA damage.

Influence of the amount of DNA during irradiation on the cell survival curve

According to the above-mentioned irradiation design (Fig. 2), we evaluated the cell survival curves for two dose rates: 0.186 and 1.00 Gy/h. The survival curve for fractionated irradiation was determined by Eq. 11 including the change in the amount of DNA is shown in Fig. 5 (hereafter, we denote this the MK-DNA model), while the curve not including the change in the amount of DNA was determined by Eq. 12 (hereafter the MK-previous model). Figure 6a and b show comparisons between the curves for the MK-DNA model (solid line) and the MK-previous model (dotted line) together with experimental survival data (symbols) for 0.186 Gy/h (report by Metting *et al.* [34]) and 1.00 Gy/h (our work). In addition, as shown in Fig. 6c, we also evaluated the survival curve for 1.50 Gy/h (the closest dose rate to 1.00 Gy/h used in this study) by comparing it with the continuous irradiation data of Metting *et al.* [34]. The curves for the two models for 1.50 Gy/h were calculated in the same manner as for 1.00 Gy/h. To demonstrate continuous irradiation, the time interval ΔT was set to be 1/10 h.

Over a large absorbed dose range, the surviving fraction described by the MK-DNA model featured a higher radiosensitivity than that described by the MK-previous model. As listed in Table 2, the χ^2 (χ^2_S, $\chi^2_{-\log S}$) values obtained with the MK-DNA model for 1.00 and 1.50 Gy/h are smaller than those obtained with the MK-previous model. Inversely, the values obtained with the MK-DNA model for 0.186 Gy/h are not smaller than those obtained with the MK-previous model. This discrepancy is represented by difference in the surviving fractions in the higher dose region, as shown in Fig. 6a. Contrary to this, the cell survival curves for the dose rates with 1.00 and 1.50 Gy/h can be favorably reproduced by incorporating the amount of DNA modulated by the accumulation of cells in G_2. Under protracted irradiation such as 0.186 Gy/h, there is a possibility that other factors such as cell proliferation [21, 40, 41] and adaptive response [42, 43] affect the surviving fraction. Further investigations are necessary on this point with regard to lower-dose-rate exposure. Nevertheless, in terms of the χ^2 values for the three dose rates, the estimation fidelity of the MK model was improved,

Table 2. Comparison of the MK model with and without change in the amount of DNA per cell nucleus

Dose rate	Change in amount of DNA (type of the MK model)	χ^2-values (survival)	χ^2-values (−log of survival)
0.186 Gy/h	Increase → Saturated (MK-DNA model)	0.022	0.090
	Constant (MK-previous model)	0.017	0.062
1.00 Gy/h	Increase → Saturated (MK-DNA model)	0.254	1.102
	Constant (MK-previous model)	0.304	1.694
1.50 Gy/h	Increase → Saturated (MK-DNA model)	0.019	0.117
	Constant (MK-previous model)	0.037	0.213
Total	MK-DNA model	0.295	1.309
	MK-previous model	0.358	1.968

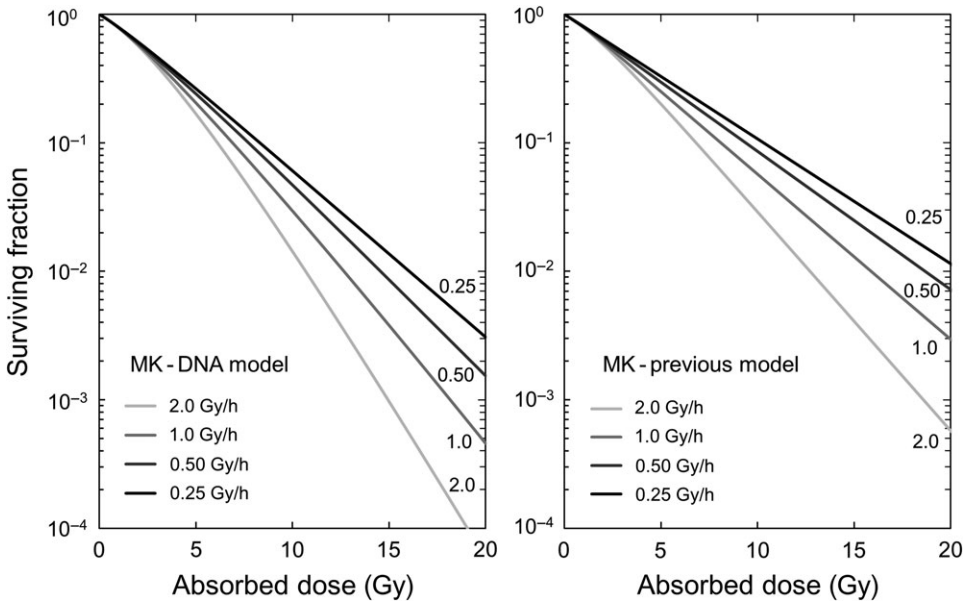

Figure 7. Estimated dose-rate effects from the MK-DNA model in comparison with the previous MK model. The change of DNA amount during the irradiation at 1.00 Gy/h (solid line in Fig. 5) was used for estimating the cell survival curves for various dose rates, and the surviving curves were calculated by Eq. 11 in the MK-DNA model. The numbers in this figure represents the dose rate (in Gray per hour).

as shown in the total χ^2 values in Table 2. The change in amount of DNA per nucleus should be taken into consideration when predicting the characteristics of cell fate after protracted exposure.

Evaluation of the dose-rate effects correlated with accumulation of cells in G_2 and HRS

To see the influence of the amount of DNA on the characteristic curves for the DREs (Fig. 5), we estimated the cell survival curves for various dose rates ranging from 0.25 to 2.0 Gy/h. These dose rates might have caused accumulation of cells in G_2. The surviving fraction was estimated with the use of increasing DNA condition under 1.00 Gy/h irradiation, and the survival curves were described by the MK-DNA model ($\dot{D}\Delta T = 0.1$ Gy) for various dose rates. Figure 7 shows the estimated DREs of the cell survival curve for four dose rates between 0.25 and 2.0 Gy/h, where HRS was confirmed by comparing the surviving fractions by the MK-DNA model with those by the MK-previous model.

In the MK-DNA model expressed in Eq. 11, the amount of DNA in the cell population was incorporated into the model by the parameters $\langle G_n \rangle$ and $\langle G_n \rangle^2 \Phi_n$. The number of PLLs increased due to an increase in the amount of DNA in the cell nucleus. As the result of DNA damage enhancement, the MK-DNA model indicated a higher radiosensitivity than indicated by the MK-previous model. In addition, this demonstration evoked a hypothesis that the increase in PLLs due to accumulation of cells in G_2 may induce a lot of miss-

rejoining of DNA and chromosomal aberrations under protracted irradiation. Whether this is the case or not, the change in amount of DNA per nucleus during irradiation appears to be one of the important factors for inducing HRS when irradiation times become longer.

Although other factors for inducing HRS (such as disorder of the DNA repair mechanisms and non-targeted effect) are not discussed in this study, we deduced the relationship between accumulation of cells in G_2 and higher radiosensitivity from a combination of biological experiments and a theoretical approach based on a mathematical model. Previously, it was reported that the CHO-K1 cell line rarely shows low-dose HRS [13]. However, in the case of protracted irradiation, HRS was observed in experiments and this feature was interpreted by the mathematical model. The model used in this study may be able to describe the cell survival curves more faithfully by including HRS in the high dose range. Hence, the MK-DNA model may contribute not only to the evaluation of effects on the human body of long-term exposure to radiation, but also to accuracy in prediction of cell-killing in radiotherapy such as brachytherapy.

CONCLUSION

In this study, we investigated the contribution of the accumulation of cells in G_2 during protracted irradiation to determining the surviving fraction of cells exposed to 250 kVp X-rays. To demonstrate protracted continuous irradiation, an equivalent multifractionated irradiation scheme was applied to a population of CHO-K1 cells. The approximate design was validated by using a theoretical approach in the form of the MK model, which showed that a fractionated regimen with pulsed irradiation is equivalent to continuous irradiation. The amount of DNA per nucleus was quantified by flow cytometric analysis with PI; the experimental results showed a subtle accumulation of cells in G_2 under 0.186 Gy/h and a noticeable accumulation under 1.00 Gy/h. We modified the MK model so as to incorporate the amount of DNA per nucleus during irradiation (the MK-DNA model). The MK-DNA model, which considered the change of DNA amount per nucleus during irradiation, reproduced experimental clonogenic survival data with good agreement. In addition, the MK-DNA model in the high dose range featured a higher radiosensitivity than the previous MK model. Under the conditions of a notable accumulation of cells in G_2 during protracted irradiation, the dose-rate effects might be affected by modulation of the amount of DNA per nucleus during irradiation. Changes in the amount of DNA per nucleus due to cell accumulations in G_2 are possibly related to HRS in the high dose range.

FUNDING

This work was supported by JSPS KAKENHI (Grant Number 16J07497). Funding to pay the Open Access publication charges for this article was provided by Hiroyuki Date (Faculty of Health Sciences, Hokkaido University).

ACKNOWLEDGEMENTS

We would like to thank Kenneth L. Sutherland Ph.D. (Graduate School of Medicine, Hokkaido University, Sapporo, Japan), who kindly allocated time for the English proofreading of the manuscript.

CONFLICT OF INTEREST

No actual or potential conflicts of interest exist for any of the authors.

REFERENCES

1. High Level and Expert Group (HLEG). *Final report of High Level and Expert Group on European Low Dose Risk Research*, 2009 (http://www.hleg.de/fr.pdf) (20 August 2016, date last accessed).
2. Nagasawa H, Little JB. Induction of sister chromatid exchanges by extremely low doses of α-particles. *Can Res* 1992;52:6394–6.
3. Nagasawa H, Little JB. Unexpected sensitivity to the induction of mutations by very low doses of alpha-particle radiation: evidence for a bystander effect. *Radiat Res* 1999;152:552–7.
4. Brian M, Spencer JC. Low-dose hyper-radiosensitivity: past, present, and future. *Int J Radiat Oncol Biol Phys* 2008;70:1310–8.
5. Tauchi H, Endo S, Eguchi-Kasai K, et al. Cell cycle and LET dependence for radiation-induced mutation: a possible mechanism for reversed dose-rate effect. *J Radiat Res* 1999;40(Suppl):S45–52.
6. Joiner M, van der Kogel AJ. The dose-rate effect. In: Joiner M, van der Kogel AJ (eds). *Basic Clinical Radiobiology*. London: Hodder Arnold; 2009,158–68.
7. Amundson SA, Chen DJ. Inverse dose-rate effect for mutation induction by γ-rays in human lymphoblasts. *Int J Radiat Biol* 1996;69:555–63.
8. Stevens DL, Bradley S, Goodhead DT, et al. The influence of dose rate on the induction of chromosome aberrations and gene mutation after exposure of plateau phase V79-4 cells with high-LET alpha particles. *Radiat Res* 2014;182:331–7.
9. Mitchell CR, Folkard M, Joiner MC. Effects of exposure to low-dose-rate ^{60}Co gamma rays on human tumor cells *in vitro*. *Radiat Res* 2002;158:311–8.
10. Marples B, Wouters BG, Collis SJ, et al. Low-dose hyper-radiosensitivity: a consequence of ineffective cell cycle arrest of radiation-damaged G_2-phase cells. *Radiat Res* 2004;161:247–55.
11. Rothkamm K, Löbrich M. Evidence for a lack of DNA double-strand break repair in human cells exposed to very low X-ray doses. *Proc Natl Acad Sci U S A* 2003;100:5057–62.
12. Collis SJ, Schwaninger JM, Ntambi AJ, et al. Evasion of early cellular response mechanisms following low level radiation-induced DNA damage. *J Biol Chem* 2004;279:49624–32.
13. Chalmers A, Johnston P, Woodcock M, et al. PARP-1, PARP-2, and the cellular response to low doses of ionizing radiation. *Int J Radiat Oncol Biol Phys* 2004;58:410–9.
14. Hamada N, Matsumoto H, Hara T, et al. Intercellular and intracellular signaling pathways mediating ionizing radiation-induced bystander effects. *J Radiat Res* 2007;48:87–95.
15. Morgan WF, Sowa MB. Non-targeted bystander effects induced by ionizing radiation. *Mutat Res* 2007;616:159–64.
16. Prise KM, O'Sullivan JM. Radiation-induced bystander signalling in cancer therapy. *Nat Rev Cancer* 2009;9:351–60.
17. Hawkins RB. A statistical theory of cell killing by radiation of varying linear energy transfer. *Radiat Res* 1994;140:366–74.
18. Hawkins RB. A microdosimetric-kinetic model of cell death from exposure to ionizing radiation of any LET, with experimental and clinical applications. *Int J Radiat Biol* 1996;69:739–55.

19. Matsuya Y, Ohtsubo Y, Tsutsumi K, et al. Quantitative estimation of DNA damage by photon irradiation based on the microdosimetric-kinetic model. *J Radiat Res* 2014;55:484–93.
20. Hawkins RB, Inaniwa T. A microdosimetric-kinetic model for cell killing by protracted continuous irradiation including dependence on LET I: repair in cultured mammalian cells. *Radiat Res* 2013;180:584–94.
21. Hawkins RB, Inaniwa T. A microdosimetric-kinetic model for cell killing by protracted continuous irradiation II: brachytherapy and biologic effective dose. *Radiat Res* 2014;182:72–82.
22. Inaniwa T, Suzuki M, Furukawa T, et al. Effects of dose-delivery time structure on biological effectiveness for therapeutic carbon-ion beams evaluated with microdosimetric kinetic model. *Radiat Res* 2013;180:44–59.
23. Okamoto H, Kanai T, Kase Y, et al. Relation between lineal energy distribution and relative biological effectiveness for photon beams according to the microdosimetric kinetic model. *J Radiat Res* 2011;52:75–81.
24. Matsuya Y, Tsutsumi K, Sasaki K, et al. Evaluation of the cell survival curve under radiation exposure based on the kinetics of lesions in relation to dose-delivery time. *J Radiat Res* 2015;56:90–9.
25. Mitchell JB, Bedford JS, Bailey SM. Dose-rate effects in plateau-phase cultures of S3 HeLa and V79 cells. *Radiat Res* 1979;79:552–67.
26. Nelson JM, Todd PW, Metting NF. Kinetic differences between fed and starved Chinese hamster ovary cells. *Cell Tissue Kinet* 1984;17:411–25.
27. Pawlik TM, Keyomarsi K. Role of cell cycle in mediating sensitivity to radiotherapy. *Int J Radiat Oncol Biol Phys* 2004;59:928–42.
28. Sinclair WK, Morton RA. X-ray sensitivity during the cell generation cycle of cultured Chinese hamster cells. *Radiat Res* 1966;29:450–74.
29. Mao Z, Bozzella M, Seluanov A, et al. DNA repair by nonhomologous end joining and homologous recombination during cell cycle in human cells. *Cell Cycle* 2008;7:2902–06.
30. Hawkins RB. The influence of concentration of DNA on the radiosensitivity of mammalian cells. *Int J Radiat Oncol Biol Phys* 2005;63:529–35.
31. Jayat C, Ratinaud MH. Cell cycle analysis by flow cytometry: principles and applications. *Biol Cell* 1993;78:15–25.
32. Brenner DJ. The linear–quadratic model is an appropriate methodology for determining isoeffective doses at large doses per fraction. *Semin Radiat Oncol* 2008;18:234–9.
33. International Atomic Energy Agency (IAEA). Absorbed dose determination in photon and electron beams. An International Code of Practice. *Technical Reports Series No. 277*: IAEA, Vienna, 1987.
34. Metting NF, Brab LA, Roesch WC, et al. Dose-rate evidence for two kinds of radiation damage in stationary-phase mammalian cells. *Radiat Res* 1985;103:204–18.
35. Bedford JS, Mitchell JB. Dose-rate effects in synchronous mammalian cells in culture. *Radiat Res* 1973;54:316–27.
36. Rühm W, Azizova TV, Bouffler SD, et al. Dose-rate effects in radiation biology and radiation protection. *Ann ICRP* 2016;45 Suppl 1:262–79.
37. Mitchell JB, Bedford JS. Dose-rate effects in synchronous mammalian cells in culture: II. A comparison of the life cycle of HeLa cells during continuous irradiation or multiple-dose fractionation. *Radiat Res* 1977;71:547–60.
38. Wouters BG, Begg AC. Irradiation-induced damage and the DNA damage response. In: Joiner M, van der Kogel AJ (eds). *Basic Clinical Radiobiology*. 4th edn. London: Hodder Arnold, 2009, 11–26.
39. Hall EJ, Giaccia AJ. Cell survival curves. In: Hall EJ, Giaccia AJ. *Radiobiology for the Radiologist.* 6th edn. Philadelphia: Lippincott Williams & Wilkins, 2006, 31–46.
40. Zips D. Tumour growth and response to radiation. In: Joiner M, van der Kogel A, (eds). *Basic Clinical Radiobiology*. 4th edn. London: Hodder Arnold, 2009, 78–101.
41. Mitchell JB, Bedford JS, Bailey SM. Dose-rate effects in mammalian cells in culture: III. Comparison of cell killing and cell proliferation during continuous irradiation for six different cell lines. *Radiat Res* 1979;79:537–51.
42. Boyden GRS. Adaptive response and its variation in human normal and tumour cells. *Int J Radiat Biol* 1999;75:865–73.
43. Sawant SG, Randers-Pehrson G, Metting NF, et al. Adaptive response and the bystander effect induced by radiation in C3H 10T1/2 cells in culture. *Radiat Res* 2001;156:177–80.